

# Temperature Dependent Memory Effects on a Drain Modulated GaN HEMT Power Amplifier

R. Marante<sup>1</sup>, L. Cabria<sup>1</sup>, P. Cabral<sup>2</sup>, J. C. Pedro<sup>2</sup> and J. A. García<sup>1</sup>

<sup>1</sup>Dpto. Ingeniería de Comunicaciones, Universidad de Cantabria, Santander, Cantabria, Spain, 39005.

<sup>2</sup>Instituto de Telecomunicações, Universidade de Aveiro, Aveiro, Portugal, 3810-193.

**Abstract** — In this paper, the impact of self heating on the linearity of a drain modulated GaN HEMT power amplifier (PA) is studied. After characterizing the frequency response of junction temperature rise to power dissipation, as well as the effect of this variable on the PA modulation profiles, the dynamic envelope trajectory, under a two-tone test signal, appears to be slightly dependent on frequency spacing. Self heating related effects are shown to be negligible in presence of other nonidealities, as the case of feedthrough. In this way, punching a vector hole in the two-tone I/Q diagram and applying memoryless digital predistortion (DPD), will allow identifying the influence of self heating effects, over adjacent channel distortion. Finally, this long-term memory effect is proved to be responsible for only a minor residual distortion in a linearized EDGE polar transmitter.

**Index Terms** — EER, GaN HEMT, linearity, polar transmitter, power amplifier, self heating, temperature.

## I. INTRODUCTION

Emerging architectures are currently under study as a solution to the critical power versus spectral efficiency trade-off in modern wireless transmitters. Based on the envelope elimination and restoration technique, EER [1], polar transmitters may be able of providing, at least theoretically, the desired linear operation with 100% efficiency. Linearity will only be constrained by second order effects determined by the supply modulation nonidealities and possible time misalignment between the amplitude and phase paths.

These distortion generation mechanisms of a polar transmitter may be classified as inherent to the architecture itself or to the nonidealities of its implementation components. In the first set we have the differential delay between the amplitude and phase paths, the limited bandwidth of the amplitude or envelope branch and the very high bandwidth required to amplify a phase-only modulated signal. In the second set we have to include the undesired nonlinearities in the drain modulating profiles of the final RF stage [2].

Since this high level amplitude modulator (where switched-mode power amplification occurs simultaneously with AM restoration) is driven by a constant-envelope phase-modulated RF signal, and the amplitude component reinserted via the drain supply biasing voltage ( $V_{dd}$ ), a nonlinear  $V_{dd}$ -to-AM modulation profile and the appearance of a parasitic  $V_{dd}$ -to-PM dependence may ruin the desired transmitter performance. In fact, when system level nonidealities are kept under control,

the transmitter residual distortion is mainly determined by the signal leakage through the gate-drain capacitance,  $C_{gd}$ , at  $V_{dd}$  values close to zero, in conjunction with an undesired current-source mode of operation at the envelope peaks [2]. This should then be compensated through some external linearization process as digital predistortion.

Unfortunately, it is known that memory effects can have a significant negative impact on the actual capability of these linearization methods. So, in this paper, we study the low frequency dynamics of the  $V_{dd}$ -to-AM and  $V_{dd}$ -to-PM profiles of a saturated GaN HEMT PA, associated to the impact of transistor junction temperature,  $T_j$ , over the modulation characteristics and the switching device self heating response.

## II. DEVICE THERMAL RESPONSE CHARACTERIZATION

In order to accurately evaluate the device temperature rise dependence on power dissipation, the parameters of the thermal network in the transistor equivalent circuit were extracted for a CGH35015FE GaN HEMT from CREE®. Using the Schottky gate-to-source diode as an embedded thermometer [3], a thermal resistance value,  $R_{th} = 5.8$  °C/W, was obtained from pulsed measurements at gate terminal with a 0.1% duty cycle. The thermal capacitance ( $C_{th}$ ) was computed from the drain current time domain evolution. The drain biasing voltage was fixed at  $V_{DS} = 28$  V, the value later selected for the design of the switched-mode PA, while the gate voltage was conveniently pulsed setting two values over the pinch-off condition, in order to avoid gate lag effects, assuring an  $I_{ds}(t)$  profile determined by self heating mechanisms. The drain current evolution, captured with a digital oscilloscope, was fitted with the exponential equation of a first order thermal network, resulting in thermal constant and capacitance values of  $\tau_{th} = 13$   $\mu$ s and  $C_{th} = 2.24$   $\mu$ J/°C, respectively.

## III. SELF HEATING EFFECTS ON A DRAIN MODULATED PA

### A. AM and PM profiles as a function of temperature

The modulation profiles of a saturated GaN HEMT PA, working at 900 MHz and designed with the previously mentioned device, were then characterized at different values of case temperature, using the test set-up shown in Fig. 1.

$V_{dd}$  was swept between 0 and 35 V with the aid of a CW modulating signal, with a repetition frequency well above the cutoff value of the thermal network ( $f_{th} = 12.24$  kHz), but within the envelope path amplification bandwidth. In this way, the average dissipated power enabled the computation of the temperature difference between junction and case, which is due to the device thermal resistance. The envelope and the phase modulated paths were synchronized with the aid of the available digital delay control on the externally triggered mode of Agilent ESG Vector Signal Generators.

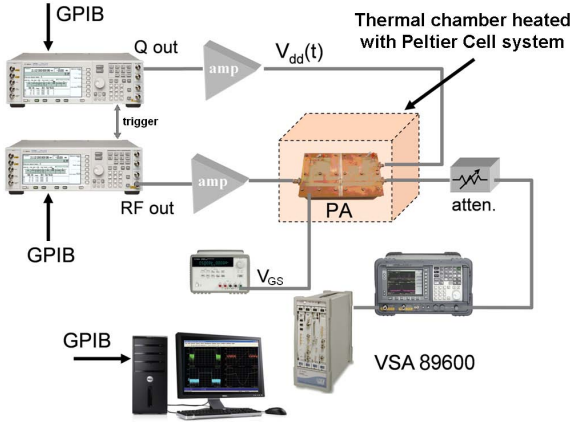


Fig. 1. Test set-up for saturated PA drain modulation characterization with junction temperature.

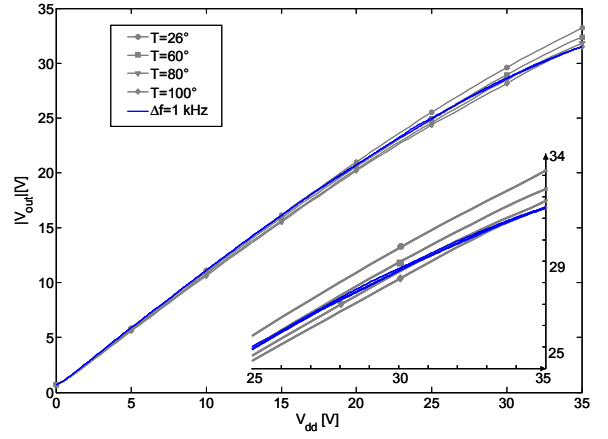
In order to obtain the complete amplitude and phase profiles in real operation regime, the output signal was captured by a vector signal analyzer. In Fig. 2, the measured  $V_{dd}$ -to-AM characteristics are plotted for a  $T_j$  range between 26°C and 100°C which leads to the conclusion that temperature rise mainly induces an additional compression in the output amplitude for high  $V_{dd}$  values.

### B. Temperature contribution to memory effects

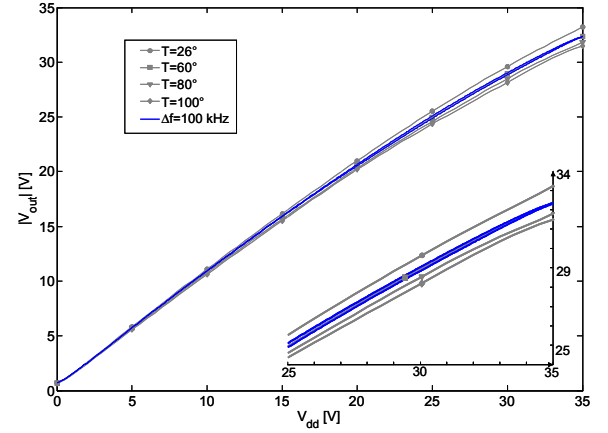
In order to gain insight into the output stage impact on polar transmitter linearity, and in particular on the possible contribution from self heating dynamics, simulations were carried out for a two-tone excitation. The frequency spacing was varied from quite below up to quite over the thermal network cutoff frequency.

First, a numeric solution for  $T_j(t)$  evolution was obtained, combining the thermal network transfer function and the characterized RF PA dissipated power dependence both on  $V_{dd}$  and  $T_j$ . The temperature influence on the  $V_{dd}$ -to-AM and  $V_{dd}$ -to-PM profiles then allowed predicting the dynamic modulation trajectory for each case (see Fig. 2 for details).

For a low frequency spacing of 1 kHz, the dynamic trajectory crosses the  $V_{dd}$ -to-AM curves at the envelope peaks. This is due to the fact that the device junction temperature may follow the time domain variations in dissipated power. At 100 kHz, however, the temperature is not able to vary at the dissipated power rate and the dynamic path approximately coincides with the curve for the average value (60°C).



a)



b)

Fig. 2. Dynamic modulation trajectories for a two-tone signal with a)  $\Delta f = 1$  kHz and b)  $\Delta f = 100$  kHz, superimposed over the  $V_{dd}$ -to-AM profiles vs.  $T_j$ .

In Fig. 3, the evolution with tone spacing is also depicted for in-band third order ( $2f_1-f_2$  and  $2f_2-f_1$ ) and fifth order ( $3f_1-2f_2$  and  $3f_2-2f_1$ ) output frequency components. Only small amplitude variations and asymmetries are appreciated, as it will be later on supported by measurements.

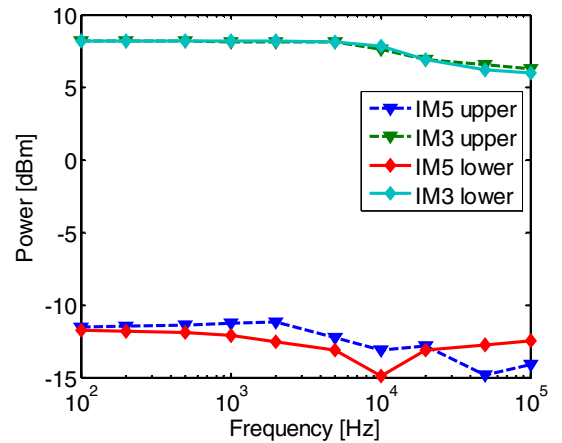


Fig. 3. Evolution of the 3<sup>rd</sup> and 5<sup>th</sup> order output components with tone spacing as obtained from simulations.

Despite the expected differences in the envelope peaks, the static nonlinearities in the  $V_{dd}$ -to-AM and  $V_{dd}$ -to-PM profiles, associated to the undesired feedthrough and current source mode of operation, seem to mask the secondary role of device self heating.

### C. Self heating impact on polar transmitter predistortion

In order to unveil the real influence of thermal dynamics on adjacent channel distortion, solutions should be searched for cancelling the dominant contributions originated by the modulating profile nonlinearities. Using memoryless digital predistortion, the  $V_{dd}$ -to-AM compression, appearing at high biasing voltage values, may be perfectly corrected. However, that is not possible with feedthrough, at least following a pure polar transmitter operation.

One straightforward solution, employed to improve polar transmitter linearity in the low amplitude region, is to punch a “vector hole” into the constellation diagram of the vector I/Q waveform [4], so that the magnitude of the envelope does not drop to a zero, or nearly zero, value. This technique was here applied to modify the classical two-tone linearity excitation, trying not to lose its highly appreciated discrete spectrum confinement characteristics.

Following the complex envelope equation in (1), a small single sideband component was added at the modulating frequency,  $\omega_m = \frac{1}{2}(\omega_2 - \omega_1)$ , creating a controllable amplitude imbalance between the tones, and, consequently, modifying the I/Q envelope trajectory to avoid the amplitude component to go below a certain fraction of the peak (see Fig. 4). This fraction,  $\alpha_{hp}$ , will be referred as the hole-punching factor.

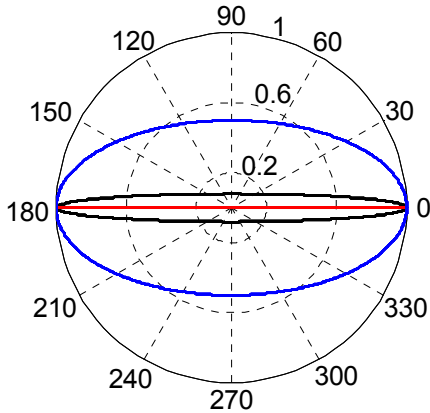


Fig. 4. Normalized I/Q trajectories in a polar diagram for the envelope of the (‘—’) original two-tone signal, together with hole-punched versions with (‘- -’)  $\alpha_{hp} = 0.08$  and (‘—’)  $\alpha_{hp} = 0.5$ .

$$x(t) = V_{dd_{max}} \cdot \left[ (1 - \alpha_{hp}) \cdot \cos(\omega_m \cdot t) + \alpha_{hp} \cdot e^{(j \cdot \omega_m \cdot t)} \right] \quad (1)$$

Using this signal, and with the aid of the test set-up of Fig. 1, the output power spectra were captured for 1 kHz and 100 kHz frequency spacing values, before and after applying digital predistortion of the  $V_{dd}$ -to-AM and  $V_{dd}$ -to-PM characteristics at a fixed junction temperature.

In Fig. 5 and Fig. 6, these results are shown for a hole-punching factor of 0.08 and 0.5, respectively.

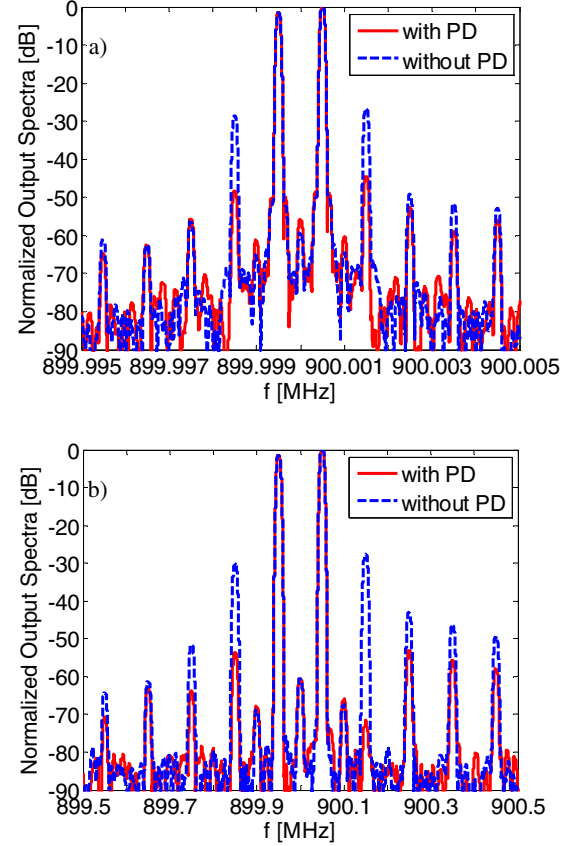


Fig. 5. Normalized output spectra after hole punching with  $\alpha_{hp} = 0.08$  for a frequency spacing of a) 1 kHz and b) 100 kHz.

The intermodulation distortion reduction, obtained with the use of digital predistortion, is evident in all cases, being the results for  $\Delta f = 100$  kHz always better than for  $\Delta f = 1$  kHz. Taking into account that 100 kHz is well above the device thermal cutoff frequency, the junction temperature is expected to remain constant along the drain voltage excursion. On the contrary,  $T_j(t)$  may perfectly follow the dissipated power variations at 1 kHz, so that the use of modulating characteristics at a fixed temperature for the applied memoryless predistortion may only lead to a moderate linearity improvement.

The observed differences are also magnified when increasing  $\alpha_{hp}$ , as the modulating voltage stays most of its period in the high  $V_{dd}$  zone, where power dissipation is higher and the AM profiles experience some noticeable dependence with temperature (as already observed in Fig. 2).

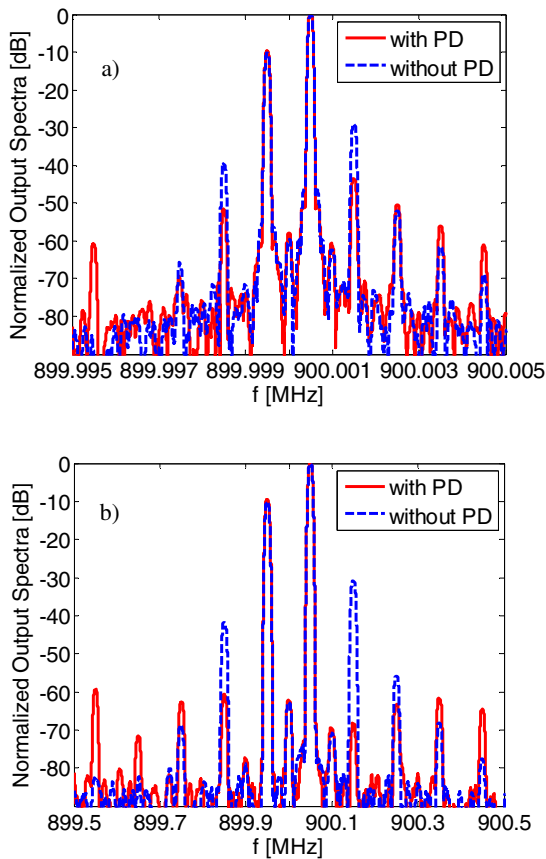


Fig. 6. Normalized output spectra after hole punching with  $\alpha_m = 0.5$  for a frequency spacing of a) 1 kHz and b) 100 kHz.

#### D. Self heating dynamics and predistortion with a real communication signal

Finally, the implemented polar transmitter was tested with a real communication signal. To avoid the impact of feedthrough while also overcoming the bandwidth limitation of the employed envelope amplifier, an EDGE excitation was selected. In Fig. 7, the measured output power spectra, with and without the use of memoryless DPD, are compared. The reduction in spectral regrowth is significant, even though a small residual distortion is still appreciable after correction. Comparing the time evolution of the measured and original complex envelopes, some minor differences were appreciated between the amplitude components in the high  $V_{dd}$  region, probably related to the impact of self heating, not taken into account during the modulating profile linearization.

Even in these conditions, a very good linearity figure of -42.5 dB normalized mean square error, NMSE, was measured. For other signals, as WCDMA or OFDM, where the envelope may go down to zero and the peak values are far from being frequent, the relative impact of this long-term memory effect is expected to be even less significant. An RF PA design optimized for efficiency would also help minimizing the influence of junction temperature dynamics.

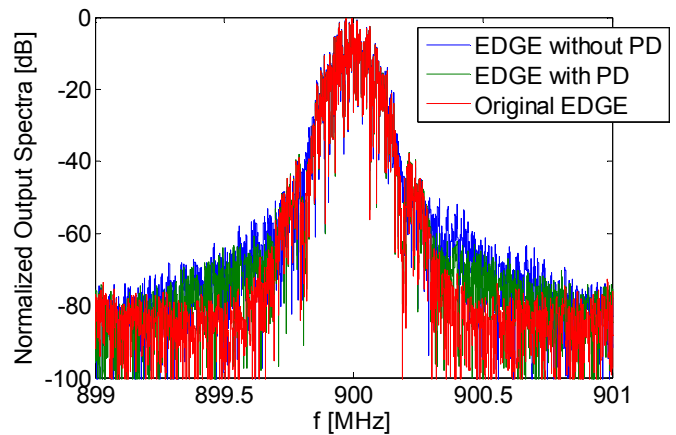


Fig. 7. Normalized measured output spectra for an EDGE signal, with and without the use of predistortion.

#### IV. CONCLUSIONS

The impact of self heating on the linearity of a drain modulated GaN HEMT PA has been studied. Starting with an extraction of the device thermal network parameters, the dynamic modulating trajectory over the  $V_{dd}$ -to-AM profiles is shown to experience some frequency dependent compression. Although the presence of static nonlinearities masks distortion contributions from thermal dynamics, self heating effects may be responsible for the residual spectral regrowth observed after applying memoryless predistortion on signals with a certain amplitude statistics.

#### ACKNOWLEDGEMENT

This work was supported by the Spanish Ministry of Science and Innovation, through projects TEC2008-06684-C03-01 and CSD2008-00068; as well as by the Portuguese Science Foundation, and Instituto de Telecomunicações, under projects PTDC/EEA-TEL/65988/2006 Digital\_PAs and SWIPA Ref. Nr.: P423, respectively. The authors appreciate the support and kind attention provided by Ryan Baker, from Cree Inc.

#### REFERENCES

- [1] L. R. Kahn, "Single-Sideband Transmission by Envelope Elimination and Restoration," *Proc. IRE*, vol. 40, no. 7, pp. 803-806, Jul. 1952.
- [2] J. C. Pedro, J. A. Garcia and P. M. Cabral, "Nonlinear Distortion Analysis of Polar Transmitters", *IEEE Trans. on Microwave Theory and Tech.*, vol. 55, no. 12, Part 2, pp. 2757-2765, Dec. 2007.
- [3] H. L. Krauss, C. W. Bostian, and F. H. Raab, *Solid State Radio Engineering*, New York: J. Wiley & Sons, 1980.
- [4] J. Wang, A. Zhu, X. Zhu and T. Brazil, "Vector Hole Punching Technique for OFDM Signals using Circle-Tangent Shift and Unused Tones", *IEEE Trans. on Microwave Theory and Tech.*, vol. 57, no. 11, pp. 2682-2691, Nov. 2009.